Carbohydrate Research 357 (2012) 32–40

Contents lists available at SciVerse ScienceDirect

Carbohydrate Research

journal homepage: www.elsevier.com/locate/carres

Self-assembling properties of 6-*O*-alkyltrehaloses under aqueous conditions

Manami Kanemaru, Kazuya Yamamoto, Jun-ichi Kadokawa *

Department of Chemistry, Biotechnology, and Chemical Engineering, Graduate School of Science and Engineering, Kagoshima University, 1-21-40 Korimoto, Kagoshima 890-0065, Japan

ARTICLE INFO

Article history:
Received 20 March 2012
Received in revised form 13 May 2012
Accepted 15 May 2012
Available online 23 May 2012

Keywords:
6-*O*-Alkyltrehalose
Self-assembly
Vesicle
Lamellar plane
Micelle

ABSTRACT

In this study, we report the self-assembling properties of 6-*O*-alkyltrehaloses with different chain lengths, that is, octyl, decyl, dodecyl, tetradecyl, and hexadecyl, under aqueous conditions. The materials were synthesized from trehalose via five reaction steps. The scanning electron microscopy (SEM), transmission electron microscopy (TEM), powder X-ray diffraction (XRD), and dynamic light scattering (DLS) measurements indicated that the self-assembling property of 6-*O*-dodecyltrehalose was completely different from that of the other derivatives. The former primarily formed spherical micelles in water, which further assembled into face-centered cubic-based aggregates when dried. The latter derivatives, on the other hand, formed vesicle-type particles via the formation of lamellar-like planes, which further merged with each other, most likely by the fusion of the planes, to construct larger aggregates.

1. Introduction

Amphiphilic molecules, that is, amphiphiles, possess hydrophilic and hydrophobic moieties in the same molecule. Under aqueous conditions, amphiphiles form self-assembling aggregates with various controlled morphologies such as spherical micelles, cylindrical micelles, spherical vesicles, planer bilayers, and tubes.[1] Because amphiphiles containing carbohydrates such as glycolipids as a hydrophilic part exhibit important in vivo functions in living systems,[2] synthetic carbohydrate-based amphiphiles have been studied extensively and have been shown to exhibit a large variety of self-assembling morphologies.[1,3] For example, the self-assembling properties and applications, as surfactants, of fatty acid esters of disaccharides such as sucrose and trehalose have been studied.[4,5] Moreover, sucrose fatty acid esters have been used as effective food additives in various industries in the form of emulsifiers.[6] The self-assembling properties of sucrose fatty acid esters change, depending on the lengths and types of the fatty acid chains and have been investigated extensively.[7] In comparison, fewer studies have looked at the self-assembling properties of amphiphilic sucrose ethers, in which a sucrose residue is attached to the alkyl chains by ether linkages.[8] Because ether linkages are more stable than ester linkages in aqueous conditions, these new ether-linked carbohydrate amphiphiles can be expected to find applications as emulsifiers and additives in various food industries. Moreover, we have considered that ether-linked carbohydrate amphiphiles exhibit self-assembling properties that are different from those of ester-linked carbohydrate amphiphiles because of the simpler structure of the ether linkage and the exclusion of the possibility of hydrogen bonding by the carbonyl group. In a previous paper, we reported the self-assembling properties of a mixture of 6-*O*- and 6′-*O*-hexadecylsucroses under aqueous conditions, which were new sucrose-based amphiphiles having the structure of a sucrose residue connected with a single hexadecyl chain by an ether linkage at either the 6- or 6′-position.[9] On the basis of the results of our analysis, we had proposed the following process for the self-assembly of the mixture of sucrose ethers under aqueous conditions. The mixture primarily formed spherical micelles with a diameter of ca. 5–7 nm in water. The micelles organized in a regular manner and formed a face-centered cubic (FCC) structure during the drying of the aqueous dispersion that led to nanoparticles with a diameter of ca. 50 nm. Moreover, several numbers of the nanoparticles further assembled together to form larger aggregates.

Trehalose is a nonreducing disaccharide, in which two glucose units are linked by an α,α-1,1′-glycosidic linkage.[10] Because trehalose has been produced industrially from starch using enzymes and has become available at low costs, it can be regarded as a new renewable resource that is comparable to sucrose. Naturally occurring glycolipids containing a trehalose residue (trehalolipids) are found in nature. An example is trehalose 6,6′-dimycolate, the most reported trehalolipid, which is an α-branched-chain mycolic acid in which the 6-position of each glucose moiety is esterified.[11] Therefore, studying the synthesis and properties of new amphiphiles composed of a trehalose residue as the hydrophilic part could contribute to the development of emulsifiers and novel food additives. Although the preparation and surfactant properties of

* Corresponding author. Fax: +81 99 285 3253.
E-mail address: kadokawa@eng.kagoshima-u.ac.jp (J. Kadokawa).

0008-6215/$ - see front matter © 2012 Elsevier Ltd. All rights reserved.
http://dx.doi.org/10.1016/j.carres.2012.05.014

synthetic amphiphilic trehalose esters have been previously reported,[5] to the best of our knowledge, amphiphilic trehalose ethers have hardly been investigated.

With the above-mentioned points in mind, in this paper, we report the synthesis and self-assembly, under aqueous conditions, of a series of new trehalose-based amphiphiles, which are 6-*O*-aklyltrehaloses having different chain lengths, that is, octyl, decyl, dodecyl, tetradecyl, and hexadecyl (**mono-C8, C10, C12, C14,** and **C16**, respectively). Consequently, we found that **mono-C8, C10, C14,** and **C16** showed hierarchically self-assembling processes based on the primary formation of lamellar-like planes, leading to vesicle-type particles and their further aggregates, whereas self-assembling property of **mono-C12** was completely different from that of the others but similar to that of the previously reported mixture of 6-*O*- and 6′-*O*-hexadecylsucrose, which was, based on the FCC-based organization of the primary formed spherical micelles.

2. Results and discussion

The synthesis of amphiphilic 6-*O*-alkyltrehaloses (**mono-C8, C10, C12, C14,** and **C16**) from trehalose was carried out by the five reaction steps according to Scheme 1, which were the successive ditritylation at the 6- and 6′positions, benzylation of the other free hydroxy groups, detritylation, monoetherification at the 6-posititon, and debenzylation. Although another synthetic approach, via monotritylation instead of ditritylation was also considered, we selected the aforementioned route via the ditritylation. Because we are investigating the self-assembly of other trehalose derivatives, namely, 6,6′-di-*O*-alkyltrehaloses (the results will be reported elsewhere), as well, and these derivatives can be synthesized simultaneously with the present 6-*O*-alkyltrehaloses from the same intermediate, that is, 6,6′-di-*O*-trityltrehalose (**1**). The compound **1** was synthesized by modifying a previously published procedure.[12] Since we could not directly obtain purified **1** from the crude products containing unreacted trehalose by a simple silica gel chromatographic method, the products were once acetylated using acetic anhydride. Then, 6,6′-di-*O*-trityltrehalose hexaacetate (**1**′) was isolated from the acetylated products by silica gel chromatography, followed by deacetylation using sodium methoxide, to yield **1**. Then, procedures including benzylation, detritylation, monoetherification using alkyl bromides with different chain lengths, and debenzylation were performed, in the same manner as reported in our previous study,[9] to obtain the five 6-*O*-alkyltrehaloses (**mono-C8**, **C10**, **C12**, **C14**, and **C16**).

The structures of all the products were confirmed by ^{1}H NMR and MALDI-TOF MS measurements. Figure 1a shows the ^{1}H NMR spectrum of **mono-C8** in CD_3OD. All the signals were assignable to the structure of **mono-C8** as follows; ^{1}H NMR (CD_3OD) δ 0.80 (t, 3H, CH_3, J = 6.8 Hz), 1.14–1.32 (m, 10H, $-(CH_2)_5-CH_3$), 1.44–1.49 (m, 2H, $-O-CH_2-CH_2-$), 3.35–3.85 (m, 14H, H-2,2′,3,3′,4,4′,5,5′,6,6′, $-O-CH_2-CH_2-$), 4.996, 5.004 (2d, 2H, H-1, J = 2.8, 3.6 Hz). The mono-etherified structure was confirmed by the appearance of two doublet sets of anomeric signals (δ 4.996 and 5.004) and the integrated ratio of the signal due to the CH_3 moiety of the octyl group to the signal due to an H-1 proton of the glucose residue, which was 3:1. The MALDI-TOF MS spectrum showed a significant peak corresponding to the molecular mass of [**mono-C8**] Na^+ (found: m/z = 477.4337; calcd: m/z = 477.2312). To further confirm the structure, the product was acetylated using acetic anhydride and pyridine. The ^{1}H NMR spectrum (Fig. 1b) of the acetylated derivative in $CDCl_3$ showed that the chemical shift of the signals assignable to the H-6 protons was not changed from that before the acetylation (Fig. 1a), whereas the signals due to the

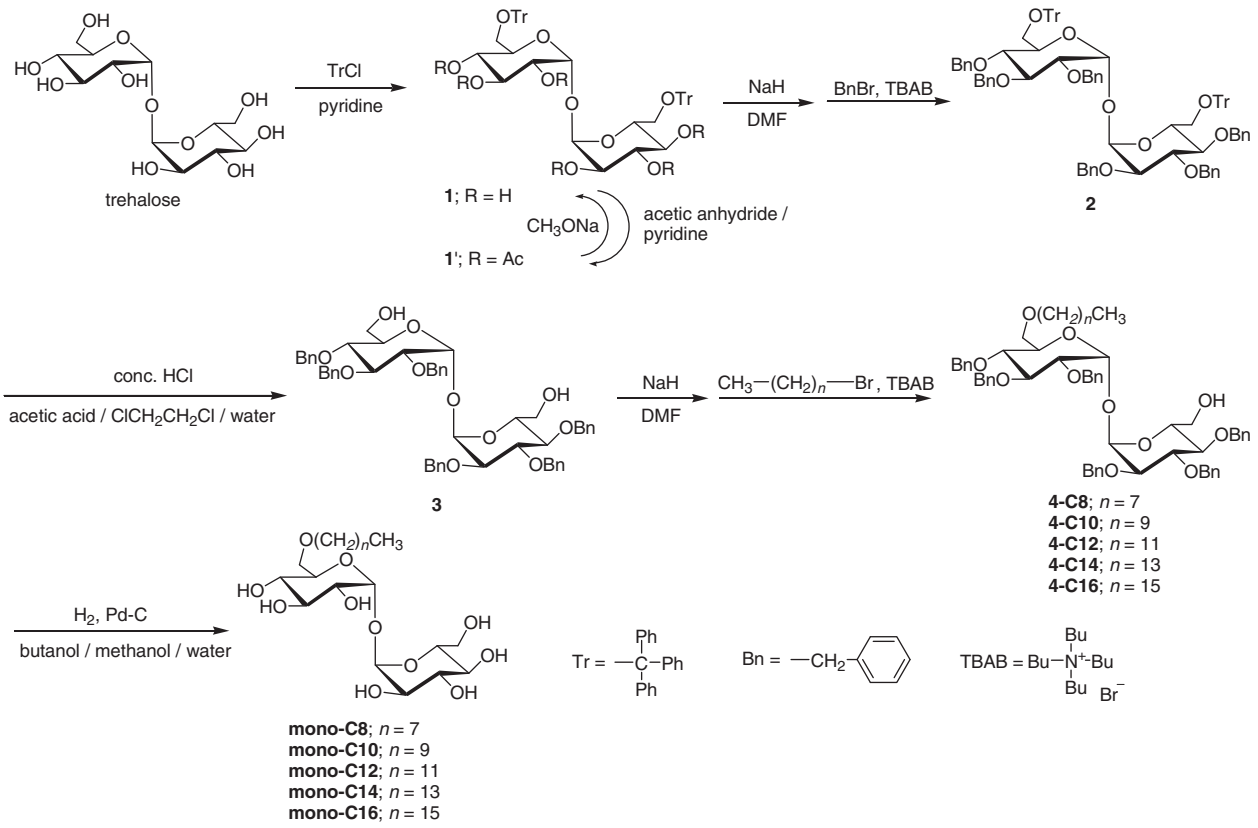

Scheme 1. Synthesis of 6-*O*-alkyltrehaloses from trehalose.

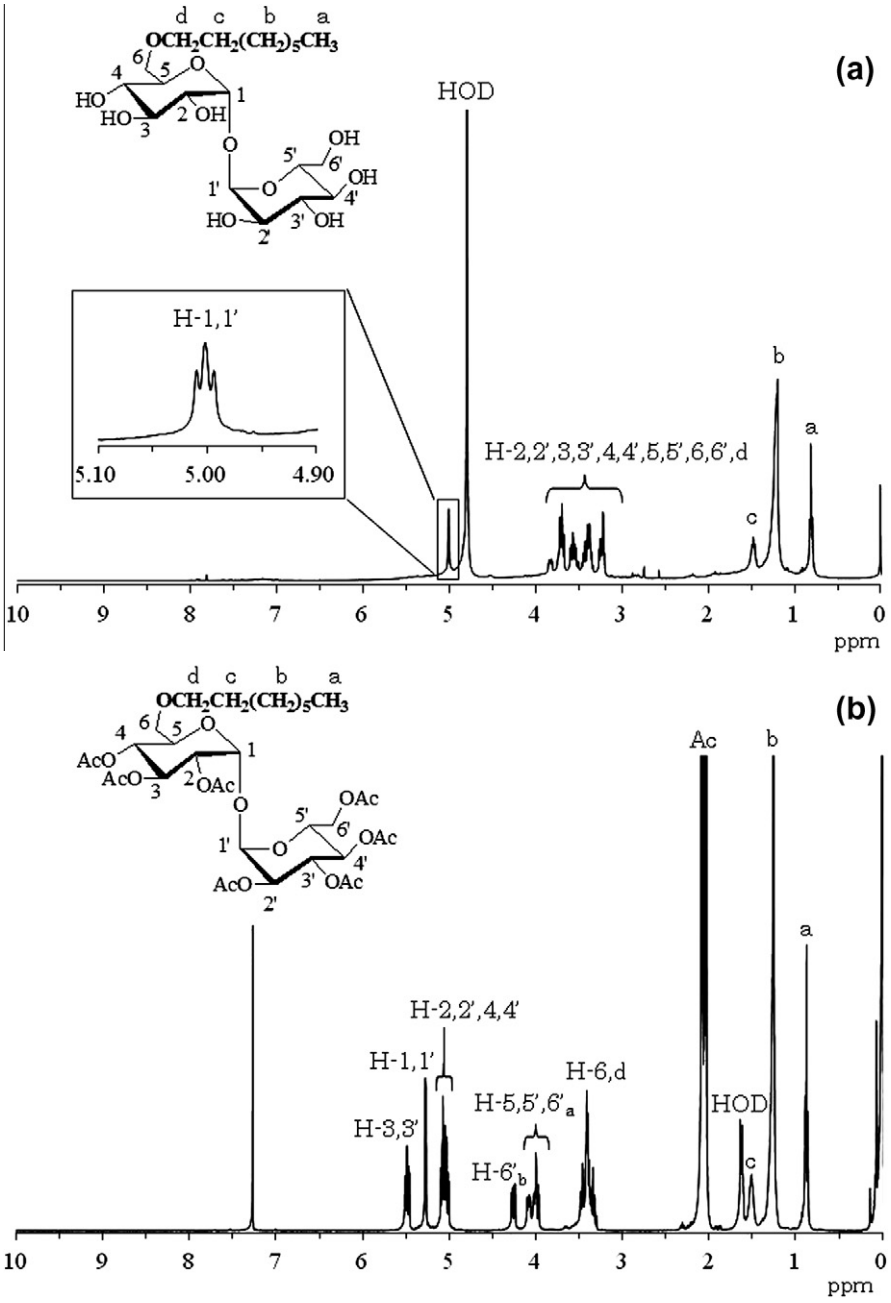

Figure 1. ^{1}H NMR spectra of (a) **mono-C8** (CD_3OD) and (b) its acetylated derivative ($CDCl_3$).

other positions (besides anomeric signals) shifted to a lower magnetic field. This data indicated that only the 6-position was etherified in the aforementioned product, and hence, was not acetylated by acetic anhydride. All the analytical and acetylation results mentioned above support the structure of **mono-C8**. The structures of the other derivatives were also confirmed in the same manner. Then, the products were subjected to the following investigations of their self-assembling properties under aqueous conditions.

In the SEM images of the samples on aluminum plates (Fig. 2), which were prepared by drying dispersions of all the derivatives in water (1.0×10^{-5} mol/L), particle-like nanoaggregates were seen. The average diameters of the aggregates of **mono-C8, C10, C14**, and **C16** decreased with an increase in the alkyl chain lengths and were 136.4, 114.1, 97.4, and 78.1 nm, respectively (the values of the standard deviations are shown in Table 1). However, the average diameter (58.3 nm) of the aggregates of **mono-C12** was smaller than that of the other aggregates, regardless of the alkyl chain length. To further confirm the hierarchical structures of the nanoaggregates, TEM measurements of the samples were performed. Dispersions of **mono-C8**–**C16** in water (1.0×10^{-5} mol/L) were placed on carbon film-coated grids. After the negative-staining technique was carried out, the TEM samples were prepared by drying the preparative materials. The TEM images of the **mono-C8, C10, C14,** and **C16** samples (Fig. 3a, b, d, and e) exhibited that several vesicle-type particles with diameters of approximately 30–60 nm assembled to form larger aggregates with sizes of approximately 80–100 nm. Furthermore, a magnified TEM image of the sample **mono-C10** (Fig. 3b′) showed that the vesicles were constructed from lamellar-like planes probably by the self-organization of the alternating hydrophilic trehalose and hydrophobic decyl layers. Interestingly, the TEM image also showed that the planes at the interfacial area between the two vesicles were fused,

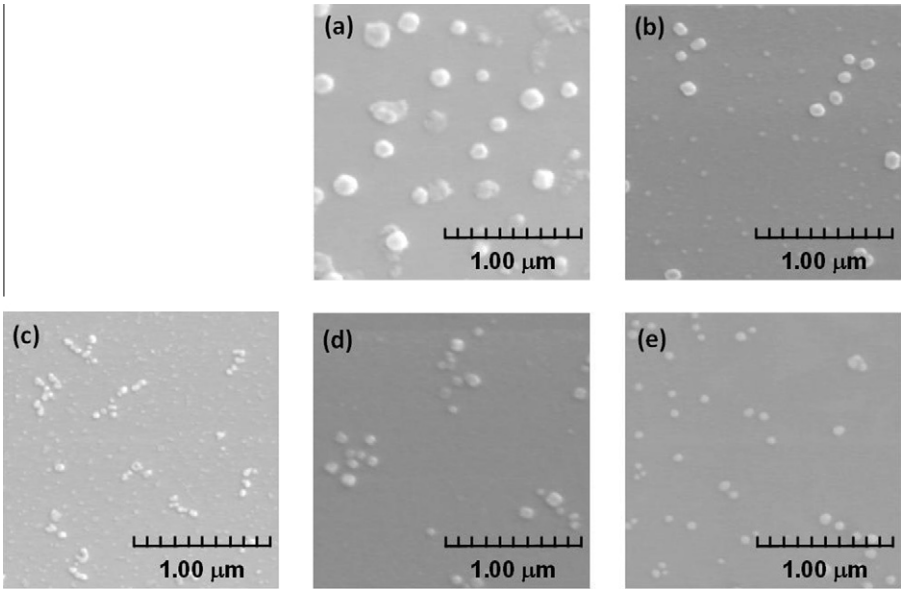

Figure 2. SEM images of the samples prepared from dispersions of (a) **mono-C8**, (b) **C10**, (c) **C12**, (d) **C14**, and (e) **C16** in water (1.0×10^{-5} mol/L).

Table 1
SEM and DLS results of 6-*O*-alkyltrehaloses

Sample	SEM results		DLS results in water (1.0×10^{-5} mol/L)	
	Average diameter (nm)	Standard deviation	Average diameter (nm)	Polydispersity index
Mono-C8	136.4	30.6	123.6	0.247
Mono-C10	114.1	22.4	123.3	0.258
Mono-C12	58.3	12.5	12.9	0.584
Mono-C14	97.4	17.5	104.4	0.730
Mono-C16	78.1	18.2	84.4	0.590

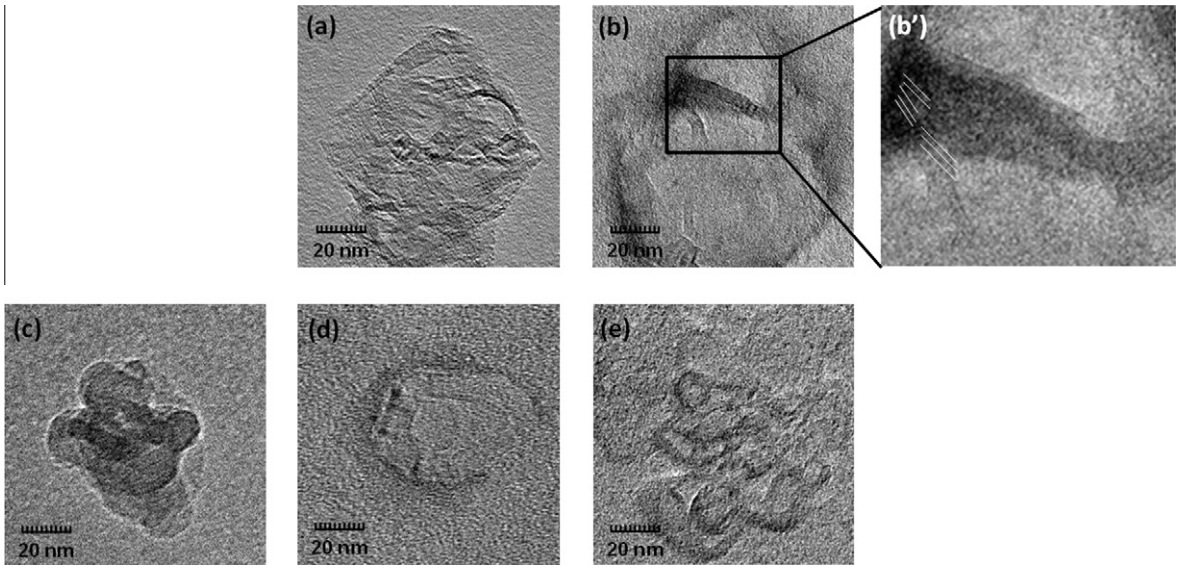

Figure 3. TEM images of the samples prepared from dispersions of (a) **mono-C8**, (b) **C10**, (c) **C12**, (d) **C14**, and (e) **C16** in water (1.0×10^{-5} mol/L) and (b′) magnified image of (b).

which probably contributed to the stabilization of the larger aggregates in water (vide section on the dynamic light scattering (DLS) measurements). On the other hand, in the TEM image of the **mono-C12** sample, some particles with diameters of approximately 15–17 nm were found to be forming aggregates with sizes of approximately 60 nm, but each particle did not exhibit a vesicle-like morphology. The SEM and TEM results suggested that the self-assembling process of **mono-C12** under aqueous conditions was different from that of the other materials under the same conditions.

To study the self-assembling processes of **mono-C8**–**C16** in even greater detail, powder X-ray diffraction (XRD) and DLS measurements were conducted. Figure 4 shows the XRD profiles of the five samples, which were prepared by drying aqueous dispersions of **mono-C8**–**C16** (1.0×10^{-3} mol/L). In the XRD profiles of the **mono-C8, C10, C14**, and **C16** samples (Fig. 4a, b, d, and e), the diffraction peaks due to (001) and further peaks assignable to the (002), (003), and/or (004) Bragg reflections of the lamellar patterns were observed.[13] From the XRD patterns, it was found that the widths of each layer increased with an increase in the alkyl chain lengths and were calculated to be 3.1 nm for **mono-C8**, 3.3 nm for **mono-C10**, 3.8 nm for **mono-C14**, and 3.9 nm for **mono-C16**. On the other hand, the XRD profile of the **mono-C12** sample (Fig. 4c) exhibited diffraction peaks ascribable to the (111), (200), and (311/222) Bragg reflections of the FCC structure.[14] Using the XRD patterns, the diameter of a sphere, which took part in the FCC structure, was calculated according to a previously described method[15] and found to be 5.1 nm. The molecular size (length) of **mono-C12** was calculated by the MM2 method using the CS Chem3D software program and found to be approximately 3 nm. Accordingly, when **mono-C12** molecules formed a spherical micelle having hydrophilic trehalose residues in the outer layer and hydrophobic dodecyl chains in the inner layer, the diameter of the sphere could be estimated to be approximately 6.0 nm, which was in good agreement with that of the sphere calculated from the XRD results. The DLS results of dispersions of all the materials in water (1.0×10^{-5} mol/L) (Fig. 5) showed monomodal profiles with relatively small polydispersity indices (Table 1). The average particle diameters of the **mono-C8, C10, C14,** and **C16** samples decreased in this order and were found to be 123.6, 123.3, 104.4, and 84.4 nm, respectively, (Fig. 5a, b, d, and e). These values were in relatively good agreement with the average diameters of the nanoaggregates observed in the SEM images. The DLS profiles and SEM/TEM images of **mono-C8, C10, C14,** and **C16** suggested that the stable nanoaggregates with diameters of around 100 nm were constructed from several vesicles by the fusion of the lamellar-like planes. On the other hand, the average particle diameter of **mono-C12** (12.9 nm) in the DLS profile (Fig. 5c) was much smaller than that observed in the SEM image (58.3 nm). The former probably corresponded to either a spherical micelle or the assembly of several micelles in the solution state, whereas the latter represented further aggregates from the micelles according to the FCC organization in the solid (dried) state.

On the basis of the above-mentioned analytical results, the following self assembling processes of the present materials are proposed (Fig. 6). The derivatives **mono-C8, C10, C14,** and **C16** form vesicle-type particles that are constructed from lamellar-like planes. The particles are further merged, most likely because of the fusion of the planes at the interfacial area between the vesicles (Fig. 6a). Therefore, the DLS profile of the aqueous dispersions of these materials showed average diameters corresponding to the merged vesicles, but to each vesicle. On the other hand, the self-assembling process of **mono-C12** under aqueous conditions is completely different from that of the other four derivatives. The self-assembly of **mono-C12** does not induce the formation of vesicle-type particles, but leads to the formation of spherical micelles in water, with a diameter of approximately 5–13 nm. These micelles are present in individual form, or only a few of which assembles in the aqueous dispersion. On the drying of the dispersion, the micelles assembled according to the FCC organization to construct the nanoaggregates with a size of approximately 60 nm (Fig. 6b). The reason for the difference in the self-assembling processes of **mono-C12** and the other derivatives is not yet clear, but it is obviously suggested that the chain lengths in 6-*O*-alkyltrehaloses strongly affect their self-assembling properties under aqueous conditions. It is likely that the balance between the hydrophilic and hydrophobic parts in **mono-C12** is more favorable for the formation of spherical micelles as compared to those in the other derivatives under aqueous conditions. More detailed studies using methods based on calculations that consider factors such as critical packing parameters are now in progress to further investigate the reasons for the difference in the self-assembling processes of 6-*O*-alkyltrehaloses, as well as to compare these reasons with the results of our previous study.[9]

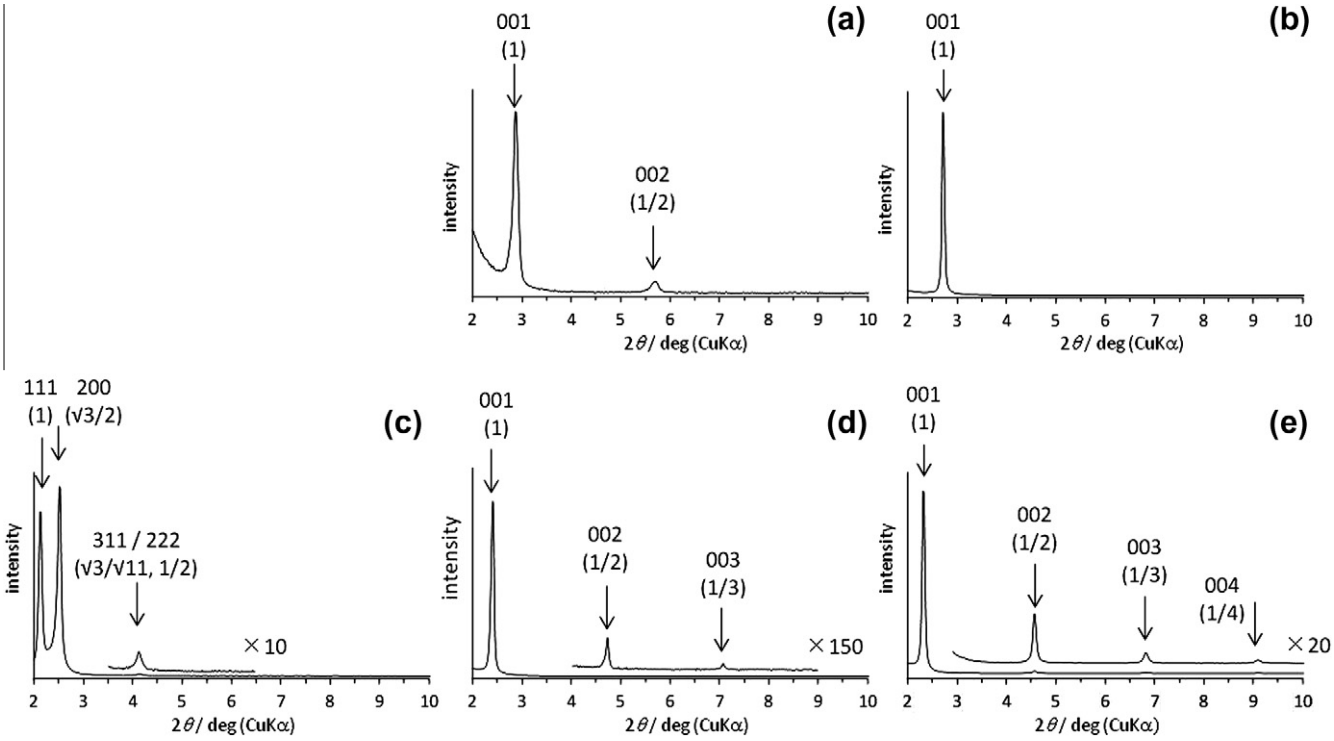

Figure 4. XRD profiles of the samples prepared from dispersions of (a) **mono-C8**, (b) **C10**, (c) **C12**, (d) **C14**, and (e) **C16** in water (1.0×10^{-3} mol/L).

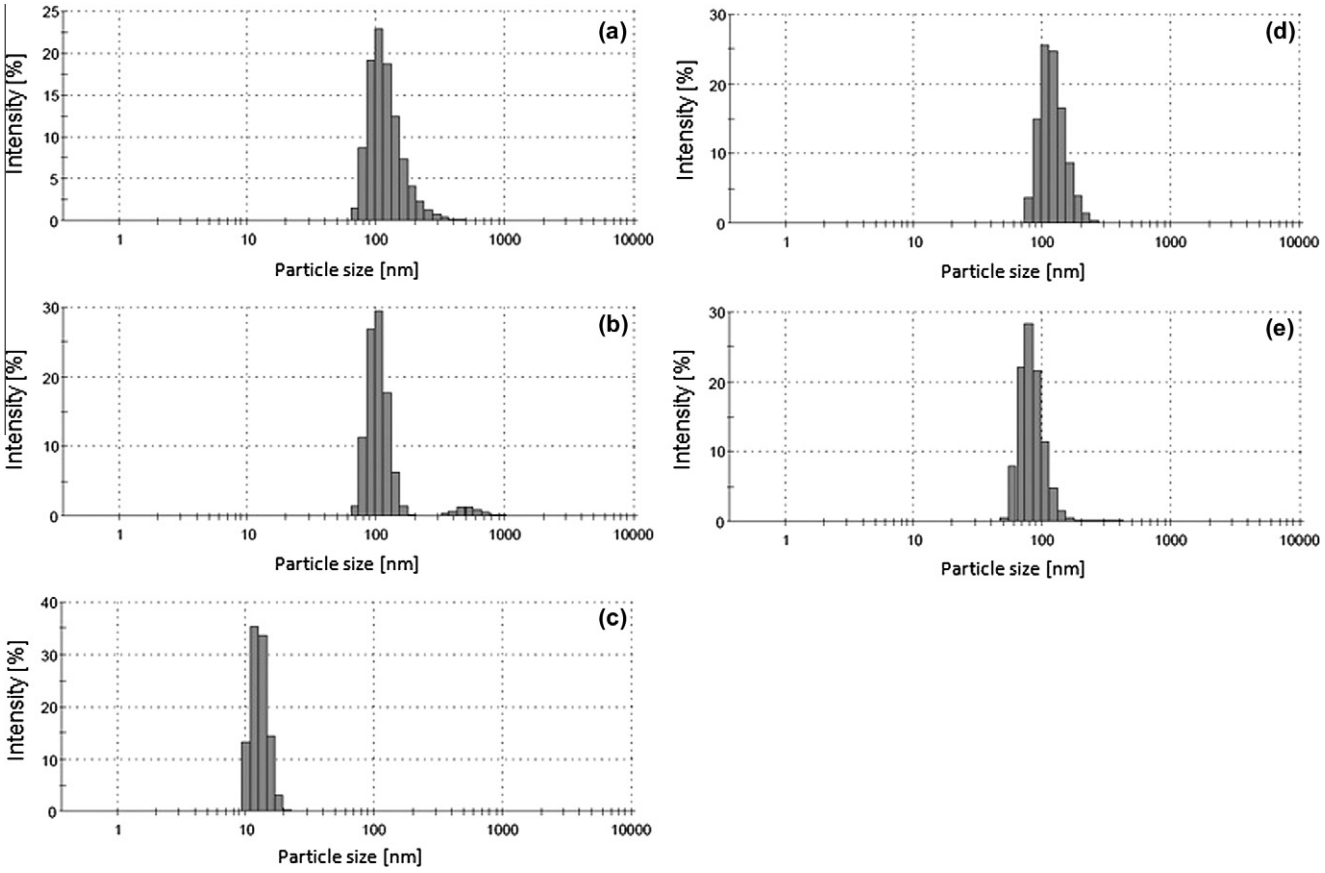

Figure 5. DLS profiles of (a) **mono-C8**, (b) **C10**, (c) **C12**, (d) **C14**, and (e) **C16** in water (1.0×10^{-5} mol/L).

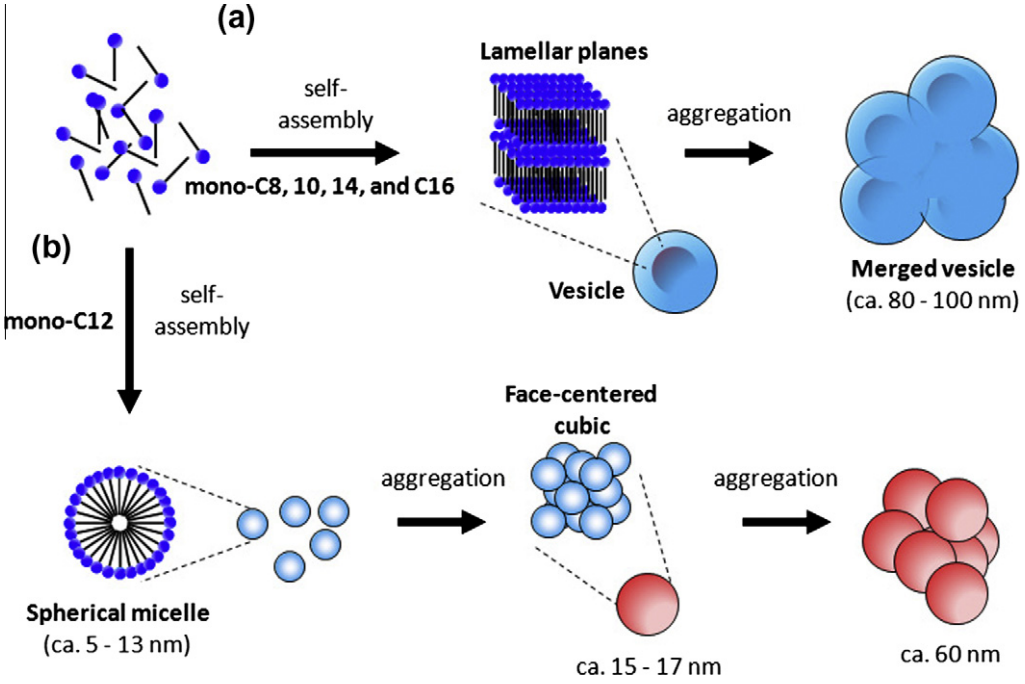

Figure 6. Plausible self-assembling processes of (a) **mono-C8, C10, C14,** and **C16** and (b) **mono-C12** under aqueous conditions.

3. Conclusion

This study investigated the characteristic processes responsible for the self-assembling properties of five 6-*O*-alkyltrehaloses (**mono-C8, C10, C12, C14**, and **C16**) with different chain lengths under aqueous conditions. The materials were synthesized from trehalose by five reaction steps. The structures of the products were established by ^{1}H NMR and MALDI-TOF MS measurements

as well as by an acetylation experiment. The self-assembling properties of the materials under aqueous conditions were evaluated using SEM, TEM, XRD, and DLS measurements. Consequently, the four materials **mono-C8, C10, C14,** and **C16** were found to form vesicle-type particles via the formation of lamellar-like planes in water. These particles merged further probably because of fusion of the planes at the interfacial area between the vesicles, to form nanoaggregates with average diameters of ca. 80–100 nm. On the other hand, **mono-C12** formed spherical micelles with a diameter of ca. 5–13 nm in water, which then assembled according to the FCC organization during the drying process from the aqueous dispersion to construct nanoaggregates with a size of ca. 60 nm. The above findings indicated that the chain lengths of the materials strongly affected their self-assembling properties under aqueous conditions. A more detailed study of the effect of the chain lengths on the self-assembling properties of the present materials is now in progress, and its results will be published in a future paper.

4. Experimental

4.1. Materials

All reagents were obtained commercially and used without further purification. *N,N*-Dimethylformamide (DMF) was purified by distillation over calcium hydride. Other solvents were used as received.

4.2. Synthesis of 6-*O*-octyltrehalose (mono-C8)

A solution of triphenylmethyl chloride (14.0 g; 50.0 mmol) in pyridine (25.0 mL) was added to a dispersion of trehalose dihydrate (3.78 g, 10.0 mmol) in pyridine (15.0 mL) at room temperature under argon and the mixture was stirred at 90 °C for 7 h. After the reaction mixture was cooled to room temperature, acetic anhydride (18.9 mL, 200 mmol) was added and the solution was stirred for 24 h at that temperature. After the mixture was coevaporated with toluene three times for concentration and diluted with chloroform, the solution was successively washed with water, dried over anhydrous Na_2SO_4, filtered, and evaporated. The residue was subjected to column chromatography using silica gel (eluent; hexane/ethyl acetate = 4:1 (v/v)) to give the **1′** (6.96 g, 6.19 mmol) in 61.9% yield. ^{1}H NMR ($CDCl_3$) δ 1.75, 1.89, 1.99 (3s, 18H, CH_3), 3.10 (d, 4H, H-6,6′, J = 3.7 Hz), 4.08–4.13 (m, 2H, H-5,5′), 5.14, 5.19 (t, dd, 4H, H-2,2′,4,4′, J = 10.8 Hz, J = 10.8, 4.4 Hz), 5.45 (t, 2H, H-3,3′, J = 9.8 Hz) 5.46 (d, 2H, H-1,1′, J = 3.6 Hz), 7.15–7.41 (m, 30H, aromatics).

Under argon, a mixture of **1′** (6.96 g, 6.19 mmol) and sodium methoxide (0.065 g, 1.02 mmol) in a mixed solvent of methanol (35.0 mL) and THF (35.0 mL) was refluxed for 5 d. After the reaction mixture was cooled to room temperature, it was treated with cation-exchange resin (Amberlite IR-120 H^+ form) for 30 min. The resin was filtered off and the filtrate was concentrated to give **1** (3.67 g, 6.45 mmol) quantitatively. ^{1}H NMR (DMSO-d_6 + D_2O) δ 3.00–4.06 (m, 12H, H-2,2′,3,3′,4,4′,5,5′,6,6′), 5.15 (d, 2H, H-1,1′, J = 3.2 Hz), 7.10–7.44 (m, 30H, aromatics).

Under argon, to a dispersion of NaH (1.63 g, 27.1 mmol) in DMF (20.0 mL) was added a solution of **1** (1.50 g, 1.81 mmol) in DMF (12.0 mL) at room temperature and the mixture was stirred at that temperature for 30 min. After benzyl bromide (1.95 mL, 16.3 mmol) and tetrabutylammonium bromide (small amount) were added to the mixture, the reaction was conducted at room temperature for 6 d. After the resulting mixture was concentrated and diluted with ethyl acetate, the solution was washed with water, dried over anhydrous Na_2SO_4, filtered, and evaporated. The residue was recrystallized from methanol/1-propanol (1:0.54 (v/v)) to give **2** (2.51 g, 1.83 mmol) quantitatively. ^{1}H NMR ($CDCl_3$) δ 3.04 - 4.24 (m, 12H, H-2,2′,3,3′,4,4′,5,5′,6,6′), 4.64–4.95 (m, 12H, CH_2-Ph), 5.46 (d, 2H, H-1,1′, J = 3.6 Hz), 6.76–7.57 (m, 60H, aromatics).

A mixture of **2** (2.37 g, 1.73 mmol) in a mixed solvent of acetic acid (5.0 mL) and 1,2-dichloroethane (5.0 mL) was refluxed for dissolution. Water (1.50 mL), 1,2-dichloroethane (5.0 mL), and concentrated hydrochloric acid (approximately 15 drops) were added, in this order, to the mixture at that temperature and the mixture was kept at that temperature for another 10 min. After the reaction mixture was cooled to room temperature and diluted with 1,2-dichloroethane, it was neutralized by the addition of saturated aqueous $NaHCO_3$ with stirring, diluted with water, and extracted with chloroform. The organic layer was dried over anhydrous Na_2SO_4, filtered, and evaporated. The residue was subjected to column chromatography using silica gel (eluent; hexane/ethyl acetate = 5:1→3:1 (v/v)) to give **3** (0.99 g, 1.12 mmol) in 64.9% yield. ^{1}H NMR ($CDCl_3$) δ 3.49–3.59 (m, 8H, H-2,2′,4,4′,6,6′), 4.04 - 4.09 (m, 4H, H-3,3′,5,5′), 4.63–5.01 (m, 12H, CH_2-Ph), 5.12 (d, 2H, H-1,1′, J = 3.6 Hz), 7.26–7.37 (m, 30H, aromatics).

Under argon, to a dispersion of NaH (0.11 g, 1.70 mmol) in DMF (15.0 mL) was added a solution of **3** (0.51 g, 0.57 mmol) in DMF (5.0 mL) at room temperature and the mixture was stirred at that temperature for 30 min. Then, 1-bromooctane (0.33 mL, 1.70 mmol) and tetrabutylammonium bromide (small amount) were added to the mixture and the reaction was allowed to proceed at 80 °C for 24 h. After the reaction mixture was diluted with water and extracted with chloroform, the organic layer was dried over anhydrous Na_2SO_4, filtered, and evaporated. The residue was subjected to column chromatography on silica gel (eluent; hexane/ethyl acetate = 40:1→10:1→5:1 → 3:1 (v/v)) to give **4-C8** (0.18 g, 0.16 mmol) in 28.9% yield. ^{1}H NMR ($CDCl_3$) δ 0.85 (t, 3H, CH_3, J = 6.8 Hz), 1.22–1.28 (m, 10H, –(CH_2)$_5$–CH_3), 1.42–1.55 (m, 2H, –O–CH_2–CH_2–), 3.25–3.70 (m, 10H, H-2,2′,4,4′,6,6′, –O–CH_2–CH_2–), 4.01–4.11 (m, 4H, H-3,3′,5,5′) 4.58–5.01 (m, 12H, CH_2-Ph), 5.16, 5.18 (2d, 2H, H-1,1′, J = 3.2, 4.0 Hz), 7.24–7.36 (m, 30H, aromatics).

To a solution of **4-C8** (0.033 g, 0.030 mmol) in a mixed solvent of butanol (4.0 mL), methanol (0.40 mL), and water (0.13 mL) was added 10% palladium on carbon (0.0155 g) and the mixture was stirred at 60 °C for 3 d under hydrogen atmosphere. The reaction mixture was then filtered, and the filtrate was evaporated and dried under reduced pressure to give **mono-C8** (0.015 g, 0.031 mmol) quantitatively. ^{1}H NMR (CD_3OD) δ 0.80 (t, 3H, CH_3, J = 6.8 Hz), 1.14–1.32 (m, 10H, –(CH_2)$_5$–CH_3), 1.44–1.49 (m, 2H, –O–CH_2–CH_2–), 3.35–3.85 (m, 14H, H-2,2′,3,3′,4,4′,5,5′,6,6′, –O–CH_2–CH_2–), 4.996, 5.004 (2d, 2H, H-1,1′, J = 2.8, 3.6 Hz); MALDI-TOF MS: Calcd $[C_{20}H_{38}O_{11}]Na^+$: m/z 477.2312. Found: m/z 477.4337.

4.3. Synthesis of 6-*O*-decyltrehalose (mono-C10)

In the same way as **4-C8**, **4-C10** was prepared from **3** in 31.4% yield. ^{1}H NMR ($CDCl_3$) δ 0.87 (t, 3H, CH_3, J = 7.0 Hz), 1.22–1.26 (m, 14H, –(CH_2)$_7$–CH_3), 1.42–1.52 (m, 2H, –O–CH_2–CH_2–), 3.27–3.70 (m, 10H, H-2,2′,4,4′,6,6′, –O–CH_2–CH_2–), 4.01–4.11 (m, 4H, H-3,3′,5,5′) 4.58–5.01 (m, 12H, CH_2-Ph), 5.16, 5.18 (2d, 2H, H-1,1′, J = 3.6, 4.0 Hz), 7.25–7.36 (m, 30H, aromatics).

Then, synthesis of **mono-C10** was carried out in the same way as **mono-C8** from **4-C10** in 87.3% yield. ^{1}H NMR (CD_3OD) δ 0.80 (t, 3H, CH_3, J = 7.2 Hz), 1.32–1.40 (m, 14H, –(CH_2)$_7$–CH_3), 1.43–1.51 (m, 2H, –O–CH_2–CH_2–), 3.35–3.85 (m, 14H, H-2,2′,3,3′,4,4′,5,5′,6,6′, –O–CH_2–CH_2–), 4.996, 5.004 (2d, 2H, H-1,1′, J = 3.2, 3.2 Hz); MALDI-TOF MS: Calcd $[C_{22}H_{42}O_{11}]Na^+$: m/z 505.2625. Found: m/z 505.7879.

4.4. Synthesis of 6-*O*-dodecyltrehalose (mono-C12)

Similarly to **4-C8**, **4-C12** was prepared from **3** in 18.0% yield. ^{1}H NMR ($CDCl_3$) δ 0.87 (t, 3H, CH_3, J = 6.8 Hz), 1.22–1.26 (m, 18H, –(CH_2)$_9$–CH_3), 1.47–1.58 (m, 2H, –O–CH_2–CH_2–), 3.23–3.70 (m, 10H, H-2,2′,4,4′,6,6′, –O–CH_2–CH_2–), 4.01–4.11 (m, 4H, H-3,3′,5,5′) 4.58–5.01 (m, 12H, CH_2-Ph), 5.16, 5.18 (2d, 2H, H-1,1′, J = 3.6, 3.6 Hz), 7.24–7.36 (m, 30H, aromatics).

The synthesis of **mono-C12** was also carried out in the same way as that of **mono-C8** from **4-C12** in 88.2% yield. ^{1}H NMR (CD_3OD) δ 0.80 (t, 3H, CH_3, J = 6.8 Hz), 1.14–1.31 (m, 18H, –(CH_2)$_9$–CH_3), 1.43–1.51 (m, 2H, –O–CH_2–CH_2–), 3.35–3.85 (m, 14H, H-2,2′,3,3′,4,4′,5,5′,6,6′, –O–CH_2–CH_2-), 4.997, 5.004 (2d, 2H, H-1,1′, J = 2.8, 3.2 Hz); MALDI-TOF MS: Calcd [$C_{24}H_{46}O_{11}$]Na$^+$: m/z 533.2938. Found: m/z 533.4905.

4.5. Synthesis of 6-*O*-tetradecyltrehalose (mono-C14)

In the same way as **4-C8**, **4-C14** was prepared from **3** in 24.7% yield. ^{1}H NMR ($CDCl_3$) δ 0.88 (t, 3H, CH_3, J = 6.6 Hz), 1.22–1.25 (m, 22H, –(CH_2)$_{11}$–CH_3), 1.42–1.60 (m, 2H, –O–CH_2–CH_2–), 3.23–3.70 (m, 10H, H-2,2′,4,4′,6,6′, –O–CH_2–CH_2–), 4.01–4.14 (m, 4H, H-3,3′,5,5′) 4.58–5.01 (m, 12H, CH_2-Ph), 5.16, 5.18 (2d, 2H, H-1,1′, J = 3.6, 3.6 Hz), 7.24–7.36 (m, 30H, aromatics).

Then, synthesis of **mono-C14** was carried out in the same way as that of **mono-C8** from **4-C14** in 83.5% yield. ^{1}H NMR (CD_3OD) δ 0.80 (t, 3H, CH_3, J = 7.2 Hz), 1.06–1.31 (m, 22H, –(CH_2)$_{11}$–CH_3), 1.46–1.50 (m, 2H, –O–CH_2–CH_2–), 3.36–3.84 (m, 14H, H-2,2′,3,3′,4,4′,5,5′,6,6′, –O–CH_2–CH_2–), 5.018, 5.024 (2d, 2H, H-1,1′, J = 3.6, 3.6 Hz); MALDI-TOF MS: Calcd [$C_{26}H_{50}O_{11}$]Na$^+$: m/z 561.3251. Found: m/z 561.5306.

4.6. Synthesis of 6-*O*-hexadecyltrehalose (mono-C16)

In the same way as **4-C8**, **4-C16** was prepared from **3** in 25.2% yield. ^{1}H NMR ($CDCl_3$) δ 0.85 (t, 3H, CH_3, J = 6.6 Hz), 1.21–1.25 (m, 26H, –(CH_2)$_{13}$–CH_3), 1.43–1.55 (m, 2H, –O–CH_2–CH_2–), 3.24–3.70 (m, 10H, H-2,2′,4,4′,6,6′, –O–CH_2–CH_2–), 4.00–4.14 (m, 4H, H-3,3′,5,5′) 4.58–5.01 (m, 12H, CH_2-Ph), 5.16, 5.18 (2d, 2H, H-1,1′, J = 3.2, 3.6 Hz), 7.25–7.36 (m, 30H, aromatics).

Then, synthesis of **mono-C16** was carried out in the same way as that of **mono-C8** from **4-C16** in quantitative yield. ^{1}H NMR (CD_3OD) δ 0.80 (t, 3H, CH_3, J = 7.2 Hz), 1.14–1.27 (m, 26H, –(CH_2)$_{13}$–CH_3), 1.46–1.50 (m, 2H, –O–CH_2–CH_2–), 3.37–3.84 (m, 14H, H-2,2′,3,3′,4,4′,5,5′,6,6′, –O–CH_2–CH_2–), 5.020, 5.026 (2d, 2H, H-1,1′, J = 4.2, 3.6 Hz); MALDI-TOF MS: Calcd [$C_{28}H_{54}O_{11}$]Na$^+$: m/z 589.3564. Found: m/z 589.9111.

4.7. Acetylation of 6-*O*-alkyltrehaloses

A typical example was as follows. Under argon, a mixture of **mono-C8** (0.0112 g; 0.025 mmol), acetic anhydride (0.25 mL), and pyridine (0.25 mL) was stirred at room temperature for 24 h. The reaction mixture was poured into a large amount of water to precipitate the product. The precipitate was dried under reduced pressure to give the acetylated product (0.0127 g, 0.017 mmol) in 67.8% yield. ^{1}H NMR ($CDCl_3$) δ 0.88 (t, 3H, –CH_2–CH_3, J = 7.0 Hz), 1.19–1.37 (m, 10H, –(CH_2)$_5$–CH_3), 1.62–1.65 (m, 2H, –O–CH_2–CH_2–), 2.04–2.10 (7s, 21H, O=C–CH_3), 3.33–3.48 (m, 4H, H-6, –O–CH_2–CH_2–), 3.97–4.08 (m, 3H, H-5,5′,6′$_a$), 4.26 (dd, 1H, H-6′$_b$, J = 12.4, 5.2 Hz), 5.00–5.10 (m, 4H, H-2,2′,4,4′), 5.28 (d, 2H, H-1,1′, J = 4.4 Hz), 5.49, 5.49 (2t, 2H, H-3,3′, J = 9.8, 10.0 Hz). Acetylations of **mono-C10**, **C12**, **C16**, and **C18** were carried out in the same way as mentioned above.

4.8. Preparation of samples for SEM measurements

A dispersion of 6-*O*-alkyltrehalose (1.0×10^{-5} mol/L) was placed on an aluminum plate and it was left standing under ambient atmosphere until water was evaporated. Then, the resulting solid sample was subjected to the measurements.

4.9. Preparation of samples for TEM measurements

A dispersion of 6-*O*-alkyltrehalose (1.0×10^{-5} mol/L) was placed on carbon film-coated copper grids. The negative-staining technique was used for TEM sample preparation. Then, the preparative material was left standing under ambient atmosphere until water was evaporated. Then, the resulting solid sample was subjected to the measurements.

4.10. Preparation of samples for XRD measurements

A dispersion of 6-*O*-alkyltrehalose (1.0×10^{-3} mol/L) was placed on a sample plate and it was left standing under ambient atmosphere until water was evaporated. Then, the resulting solid sample was subjected to the measurements.

4.11. Measurements

The ^{1}H NMR spectra were recorded using a JEOL ECX400 spectrometer. The MALDI-TOF MS measurements were performed out using a SHIMADZU Voyager Biospectrometry Workstation System Ver.5.1 with 2.5-dihydroxybenzoic acid as the matrix containing 0.05% trifluoroacetic acid under the positive ion mode. The SEM images were obtained using a Hitachi S-4100H electron microscope. TEM measurements were performed using a Jeol JEM-3010 at 200 kV. The XRD measurements were conducted using a PANalytical X'Pert Pro MPD system with Ni-filtered Cu Kα radiation (λ = 0.15418 nm). The DLS measurement was performed on a Zetasizer Nano ZS (Malvern Instruments).

References

1. Shimizu, T.; Masuda, M.; Minakawa, H. *Chem. Rev.* **2005**, *105*, 1401–1443.
2. (a) Corti, M.; Cantù, L.; Brocca, P.; Favero, E. D. *Curr. Opin. Colloid Interface Sci.* **2007**, *12*, 148–154; (b) Kitamoto, D.; Morita, T.; Fukuoka, T.; Konishi, M.; Imura, T. *Curr. Opin. Colloid Interface Sci.* **2009**, *14*, 315–328.
3. (a) Shimizu, T. *Macromol. Rapid Commun.* **2002**, *23*, 311–331; (b) Fuhrhop, J.-H.; Wang, T. *Chem. Rev.* **2004**, *104*, 2901–2937.
4. (a) Molinier, V.; Fenet, B.; Fitremann, J.; Bouchu, A.; Queneau, Y. *J. Colloid Interface Sci.* **2005**, *286*, 360–368; (b) Molinier, V.; Kouwer, P. J. J.; Fitremann, J.; Bouchu, A.; Mackenzie, G.; Queneau, Y.; Goodby, J. W. *Chem. Eur. J.* **2006**, *12*, 3547–3557; (c) Molinier, V.; Kouwer, P. J. J.; Fitremann, J.; Bouchu, A.; Mackenzie, G.; Queneau, Y.; Goodby, J. W. *Chem. Eur. J.* **2007**, *13*, 1763–1775; (d) Goodby, J. W.; Görtz, V.; Cowling, S. J.; Mackenzie, G.; Martin, P.; Plusquellec, D.; Benvegnu, T.; Boullanger, P.; Lafont, D.; Queneau, Y.; Chambert, S.; Fitremann, J. *Chem. Soc. Rev.* **2007**, *36*, 1971–2035; (e) Queneau, Y.; Chambert, S.; Besset, C.; Cheaib, R. *Carbohydr. Res.* **2008**, *343*, 1999–2009.
5. (a) Choplin, L.; Sadtler, V.; Marchal, P.; Sfayhi, D.; Ghoul, M.; Engasser, J.-M. *J. Colloid Interface Sci.* **2006**, *294*, 187–193; (b) Sun, Y.-E.; Xia, W.-S.; Tao, G.-J.; Qin, F.; Chen, J. *Eur. Food Res. Technol.* **2009**, *229*, 403–408; (c) Schiefelbein, L.; Keller, M.; Weissmann, F.; Luber, M.; Bracher, F.; Frieß, W. *Eur. J. Pharm. Biopharm.* **2010**, *76*, 342–350.
6. Kralova, I.; Sjoblom, J. *J. Dispersion Sci. Technol.* **2009**, *30*, 1363–1383.
7. (a) Hodate, Y.; Ueno, S.; Yano, J.; Katsuragi, T.; Tezuka, Y.; Tagawa, T.; Yoshimoto, N.; Sato, K. *Colloids Surf., A* **1997**, *128*, 217–224; (b) Awad, T.; Sato, K. *J. Am. Oil Chem. Soc.* **2001**, *78*, 837–842; (c) Katsuragi, T.; Kaneko, N.; Sato, K. *Colloids Surf., B* **2001**, *20*, 229–237; (d) Awad, T.; Sato, K. *Colloids Surf., B* **2002**, *25*, 45–53.
8. Queneau, Y.; Gagnaire, J.; West, J. J.; Mackenzie, G.; Goodby, J. W. *J. Mater. Chem.* **2001**, *11*, 2839–2844.
9. Kanemaru, M.; Kuwahara, S.; Yamamoto, K.; Kadokawa, J. *Carbohydr. Res.* **2010**, *345*. 2718–1722.
10. Ohtake, S.; Wang, Y. J. *J. Pharm. Sci.* **2011**, *100*, 2020–2053.
11. Franzetti, A.; Gandolfi, I.; Bestetti, G.; Smyth, T. J. P.; Banat, I. M. *Eur. J. Lipd Sci. Technol.* **2010**, *112*, 617–627.

12. Kurita, K.; Masuda, N.; Aibe, S.; Murakami, K.; Ishii, S.; Nishimura, S. *Macromolecules* **1994**, *27*, 7544–7549.
13. (a) John, G.; Jung, J. H.; Masuda, M.; Shimizu, T. *Langmuir* **2004**, *20*, 2060–2065; (b) Masuda, M.; Shimizu, T. *Langmuir* **2004**, *20*, 5969–5977.
14. Sakya, P.; Seddon, J. M.; Templer, R. H.; Mirkin, R. J.; Tiddy, G. J. T. *Langmuir* **1997**, *13*, 3706–3714.
15. (a) Klug, H. P.; Alexander, L. E. *X-ray Diffraction Procedures for Polycrystalline and Amorphous Materials*, 2nd ed.; John Wiley: New York, 1974; (b) McEuen, P. Nanostructures. In *Introduction to Solid State Physics*; Kittel, K., Ed., 8th ed.; Wiley: New York, 2004. Chapter 8.